Supporting Information

On the Suitability of Raman Spectroscopy to Monitor the Degree of Graphene Functionalization by Diazonium Salts

Krishna Sampathkumar[1,2], Valentin Diez-Cabanes[1,3#], Petr Kovaricek[1], Elena del Corro[1,$], Milan Bouša[1], Jan Hošek[3], Martin Kalbac[1], Otakar Frank[1,]*

[1] J.Heyrovsky Institute of Physical Chemistry of the CAS, v.v.i., Dolejskova 2155/3, 182 00 Praha 8, Czech Republic

[2] Central European Institute of Technology (CEITEC), Brno University of Technology, Purkyňova 123, 612 00 Brno, Czech Republic

[3] Faculty of Mechanical Engineering, Czech Technical University in Prague, Technická 4, 16 607 Prague 6, Czech Republic

[#] current address: Laboratory for Chemistry of Novel Materials, University of Mons, Place du Parc 20, B-7000, Mons, Belgium.

[$] current address: Catalan Institute of Nanoscience and Nanotechnology (ICN2), CSIC and the Barcelona Institute of Science and Technology (BIST), Barcelona, Spain.

Corresponding Author

* otakar.frank@jh-inst.cas.cz, tel: +420 266053446

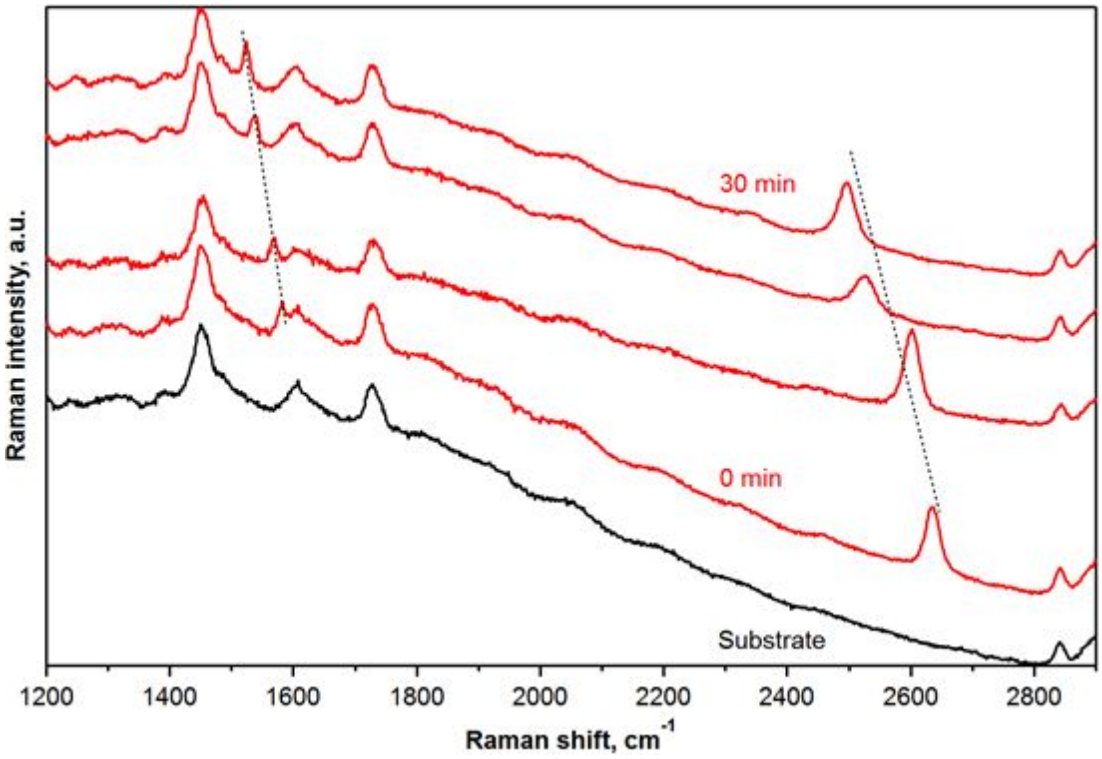

Figure S1. Raw Raman spectra of monolayer graphene (red) on PMMA-SU8 substrate (black) dipped in 1:1 methanol:water solution for increasing time, measured in the approximate center of the flake. The downshifting G and 2D bands are indicated by dashed lines.

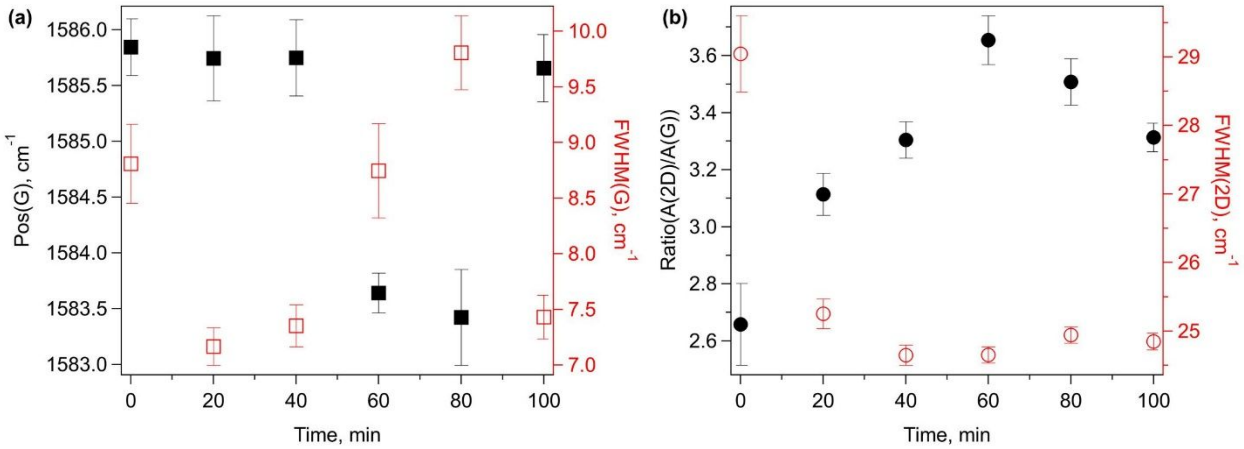

Figure S2. Blank experiment of 1L graphene on Si/SiO_2(300 nm) substrate immersed in methanol:water (1:1) solution for an indicated time. Evolution of (a) the Raman G band (shift – left axis, FWHM – right axis) and (b) area(2D/G) ratio (left axis) and FWHM(2D) (right axis), shows only minor fluctuations in part due to inhomogeneities across the flake and in part due to doping originating probably from glue remnants from the exfoliation. The data points represent average from 9 measurements, with the error bars the standard deviation.

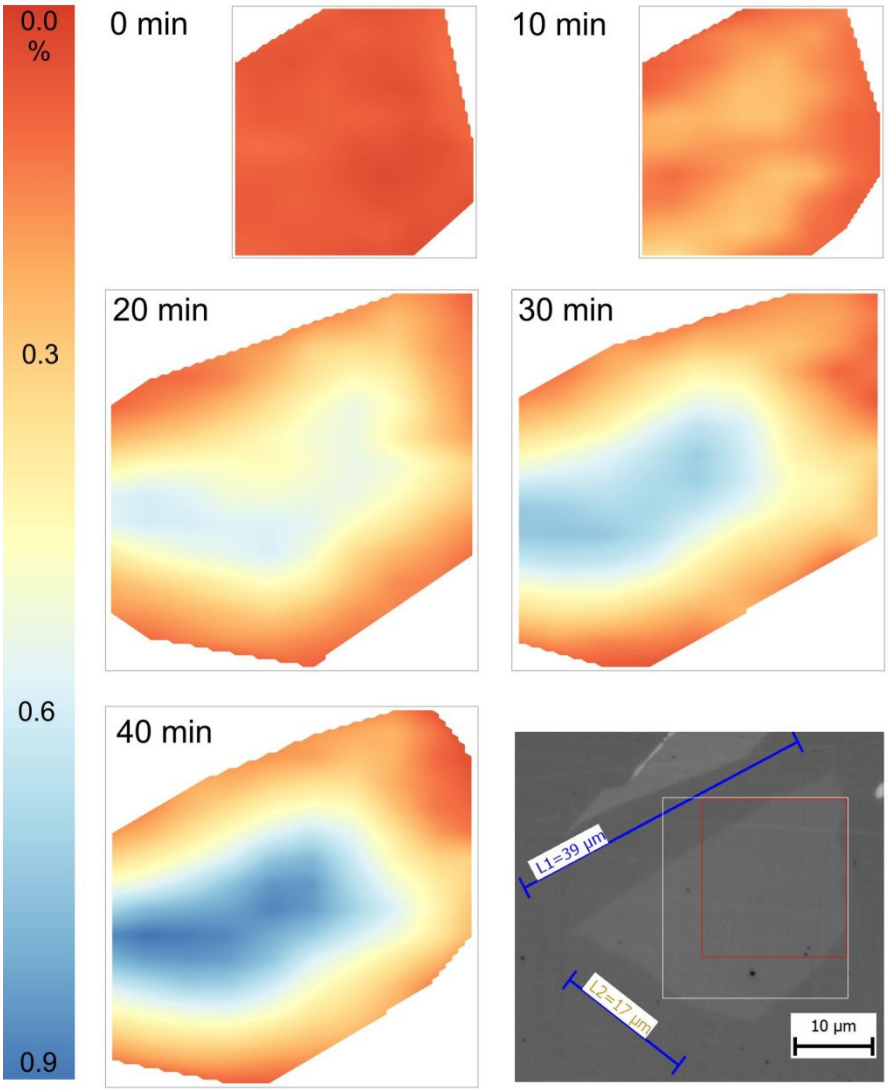

Figure S3. Evolution of the Raman spectral features of monolayer graphene on PMMA/SU8 substrate subjected to swelling in methanol:water solution. Maps of biaxial strain quantified from the 2D band shift at 0, 10, 20, 30 and 40 minutes of soaking and optical image of the flake with

the mapped area at 0 and 10 minutes (marked red), and 20, 30 and 40 minutes (white). The mapping step was 2 μm in each direction.

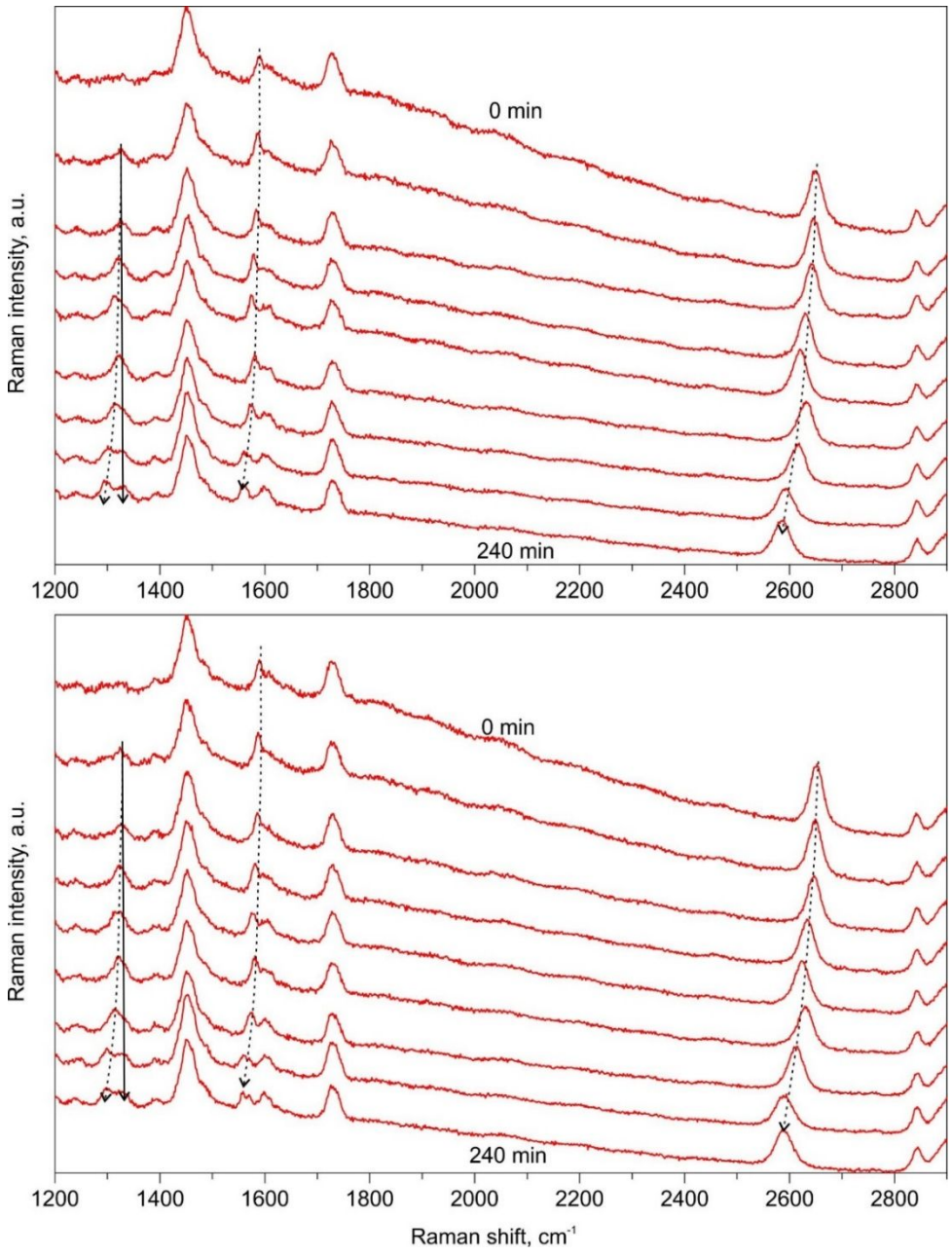

Figure S4. Evolution of Raman spectra measured at two different spots of monolayer graphene on SU8/PMMA treated with 0.01M solution (1:1 water:methanol) of 4-nitrobenzene diazonium tetrafluoroborate for 0 to 240 minutes (from top to bottom). The D, G and 2D band are marked by dashed black lines (from left to right), the v(-NO_3) vibration by solid black line. The spectra in the top panel were acquired in the approximate center of the flake, the spectra in the bottom panel approximately at half the distance between the center and the edge of the flake.

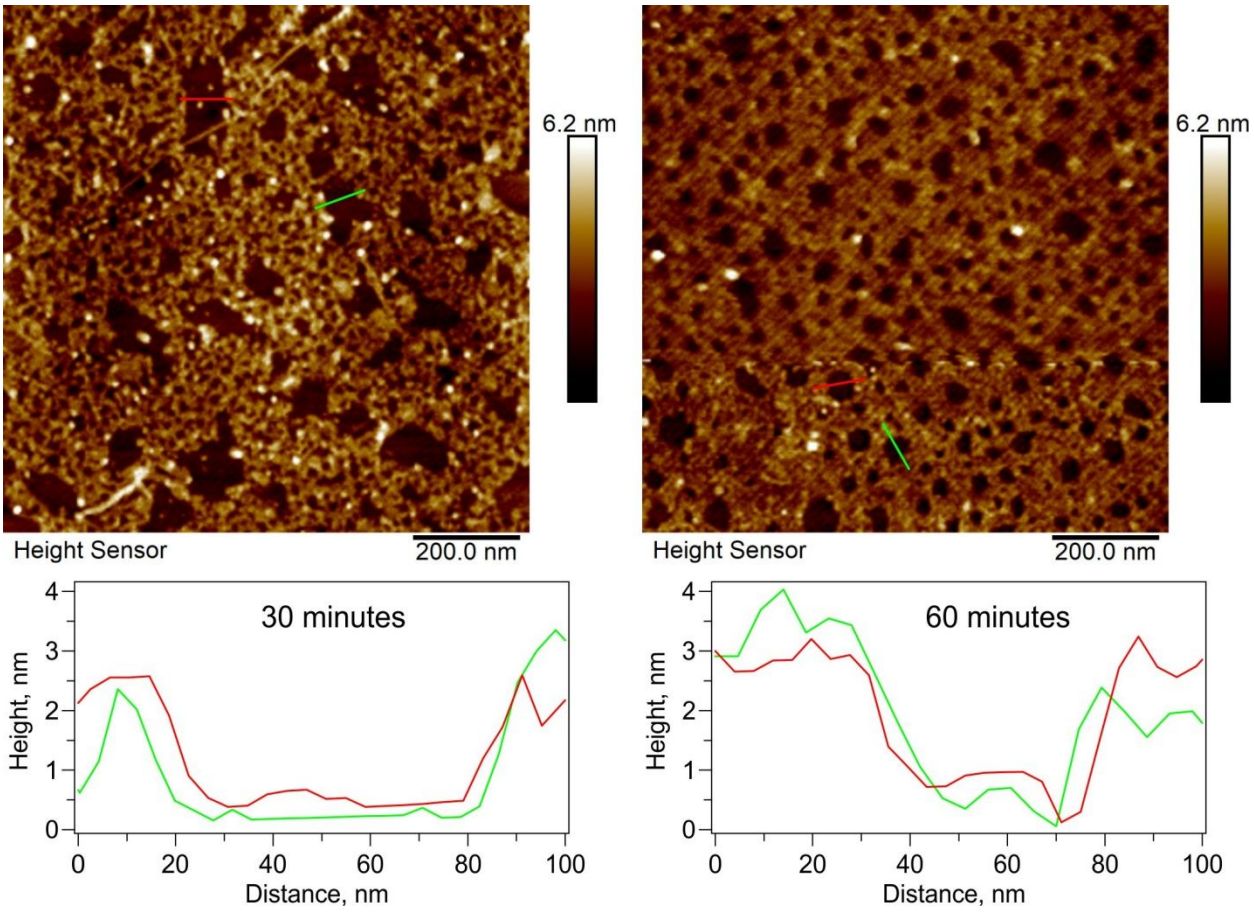

Figure S5. AFM images and extracted height profiles of monolayer graphene on SU8/PMMA treated with 0.01M solution (1:1 water:methanol) of 4-nitrobenzene diazonium tetrafluoroborate for 30 minutes (left) and 60 minutes (right). The total covered area increases from 53 to 81%,

i.e. by a factor of ~1.5. The average height difference between the covered and uncovered area is the same in both cases: 1.4 nm.

Theoretical section

Geometrical optimizations of 4-nitrobenzene diazonium compound (**1**) and its terphenyl derivative (**2**) (see Figure S6) were carried out at Density Functional Theory (DFT) level within the Becke, 3-parameter, Lee–Yang–Parr (B3LYP) functional[1] and 6-311G(d,p) basis set. The calculation of the Raman spectra was done with the same functional and basis set. In the case of the terphenyl reaction product, the vibrational properties of this compound are independent of the group attached to the central phenyl ring: hydroxy- vs methoxy- substituent (see Figure S7). For that reason, in the following discussion we consider only the first case.

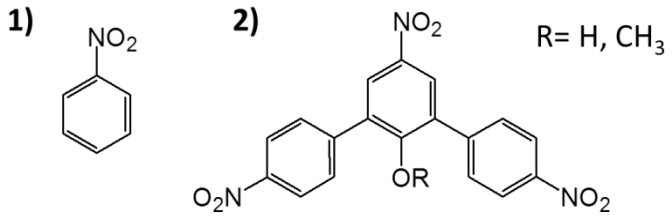

Figure S6. Chemical structures of the compounds under study.

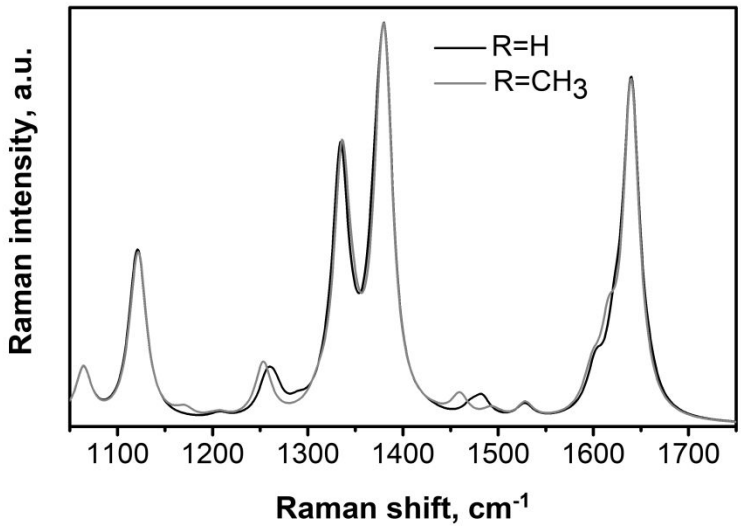

Figure S7. Calculated Raman spectra of compound **2** with hydroxy- (grey) and methoxy- (black line) substituents on the central rings as depicted in Figure S6. Note that the range of frequencies plotted (1050-1750 cm^{-1}) has been chosen in order to show the modes which are overlapping the G and D bands from garphene, whereas no important contributions to the spectra were found in the range of frequencies for graphene 2D band.

The solvent effects were introduced into our calculations by means of the Polarizable Continuum Model (PCM).[2] The calculated Raman spectra for both methanol and water solvents are identical, while a shift of ~15 cm^{-1} is induced when adding the solvent effects compared to the spectra calculated in the gas phase for both compounds (see Figure S8). This fact evidences the need of including solvent effects for a proper description of the normal modes frequencies. All theoretical calculations were performed within Gaussian16 package program,[3] whereas the Raman intensities were estimated for an

excitation wavelength of λ= 633nm and temperature T=300K by using GaussSum 3.0 plot program.[4]

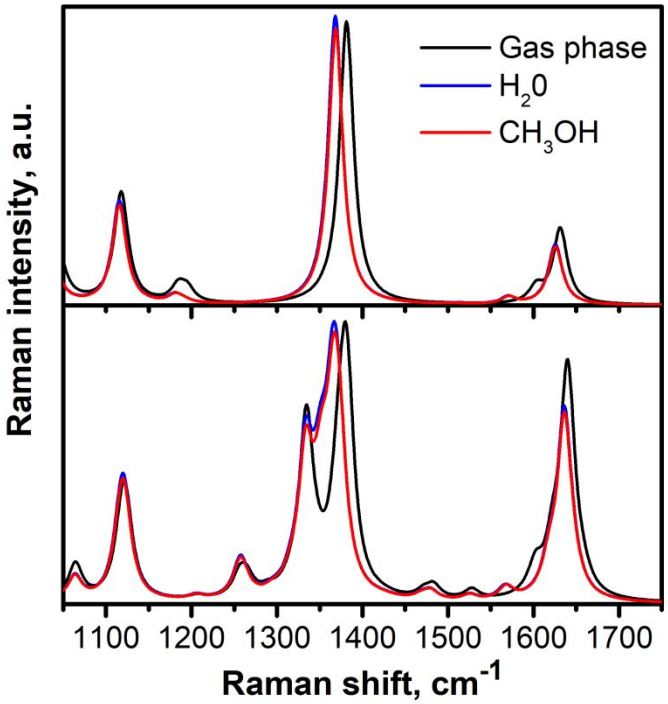

Figure S8. Calculated Raman spectra for compounds **1** (top) and **2** (bottom) for the calculations performed in gas phase (black), water (blue) and methanol (red) solvents.

The calculated Raman spectra for compounds **1** and **2** are presented in Figure S9. The spectrum of compound **1** in the region of interest is dominated by two normal modes centered at 1368 and 1625 cm^{-1}. If we compare this spectrum with the band signatures which are appearing in the measured spectra (Fig. 3, main text) as a consequence of the functionalization with NBD, we can easily attribute the above mentioned calculated modes

to the v(-NO_2) and v(C=C) vibration bands described in the main text. The small discrepancies in the absolute frequencies (the calculated spectra are ~25 cm^{-1} red-shifted with respect to the experimental frequencies) can be attributed to the facts that (i) neither the interactions with the polymer/graphene substrate nor with the neighboring molecules were included in our theoretical model and (ii) the measurement was performed on dry samples (the calculation in a solvent, which has an obvious effect on the frequencies, see above). On the other hand, the calculated spectrum of compound **2** presents the same features as the spectrum from compound **1**. In this case, the normal modes mentioned before are degenerated due to the effect of two additional nitrobenzene groups, whereas a new normal mode is appearing at 1332 cm^{-1} close to the bands attributed to the v(-NO_2) signatures.

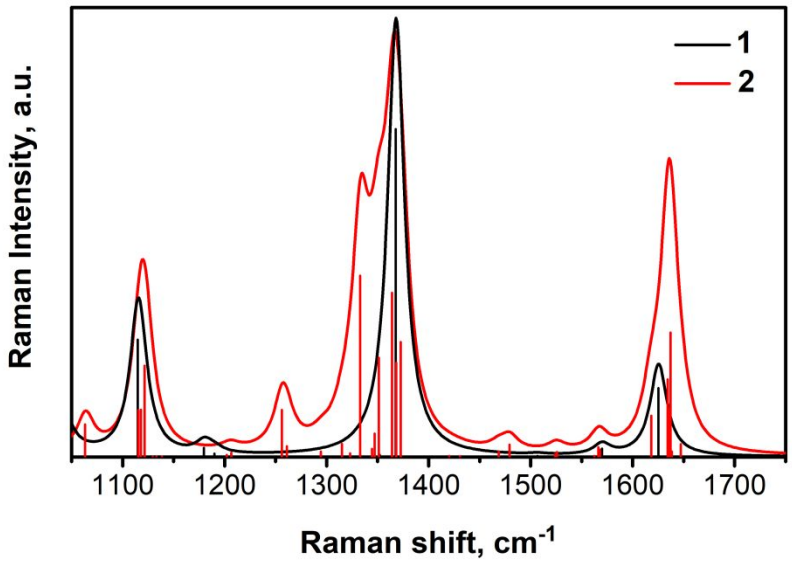

Figure S9. Calculated Raman spectra for compounds **1** (top) and **2** (bottom) in water solvent. The vertical bars represent the normalized amplitude of the Raman intensities for each normal mode.

In order to get a deeper understanding of the vibrational modes attributed to the v(-NO_2) and v(C=C) bands, we have plotted the normalized force vectors for the calculated normal modes described in the previous paragraph (see Figure S10). The vibrational mode of v(-NO_2) in compound **1** is based on the stretching mode of C-N bond for the nitro- group, which is centered at 1368 cm^{-1}. The same stretching mode is also dominating the spectra of compound **2,** in this case centered at 1364 cm^{-1}. The rest of contributions to the v(-NO_2) band in compound **2** are attributed to the stretching vibration of the N-O atoms from the nitro- group as it is the case for the normal modes centered at 1351 and 1368 cm^{-1};

and to the bending vibration of the methoxy- group which dominates the normal mode centered at 1372 cm^{-1}. In the case of the band v(C=C) band, the E_{2g} mode of the benzene core is the dominant vibration for both compounds **1** and **2**. Interestingly, for compound **2** the edge phenyl ring vibrations (centered at 1634, 1635 and 1637 cm^{-1}) present larger Raman intensities than the central ring mode (centered at 1618 cm^{-1}). Finally, we have analyzed the force vectors of normal mode which is appearing at 1332 cm^{-1} in compound **2** (Figure S11). This vibration is a combination of several modes of the benzene cores, from which we can highlight the A_{2g} mode of the edge phenyl rings.

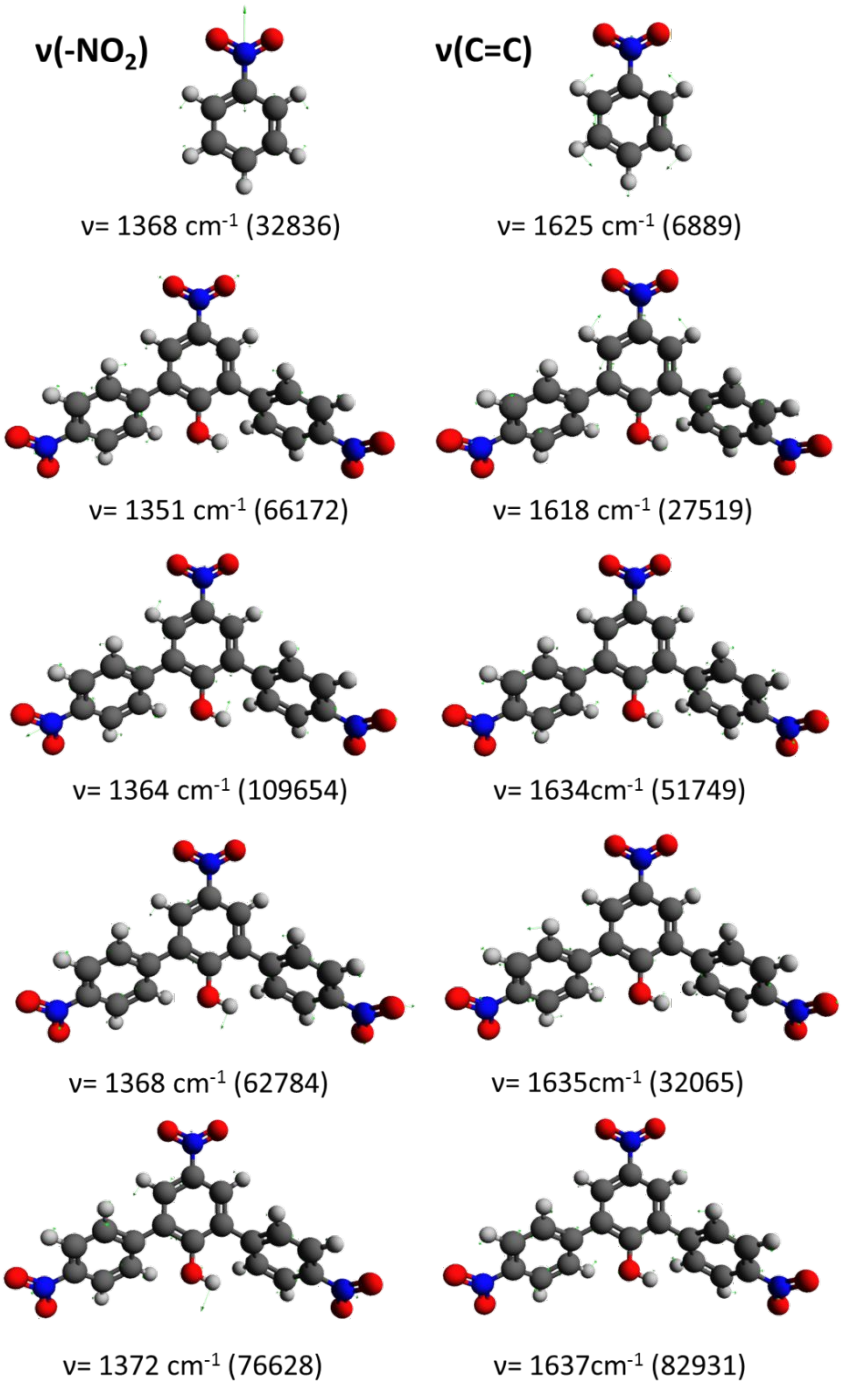

Figure S10. Normalized force vectors of the vibrational modes attributed to the ν(-NO_2) and ν(C=C) bands for compounds **1** (top) and **2** (bottom). The numbers inset represent

the frequencies and Raman intensities (in a.u. and parenthesis) for each vibrational mode.

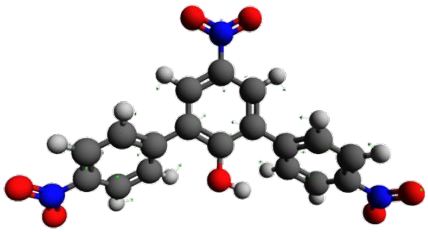

Figure S11. Normalized force vectors of the vibrational mode appearing at 1332 cm^{-1} for compound **2**. The numbers inset represent the frequencies and Raman intensities (in a.u. and parenthesis).

References

(1) Becke, A. D. Density-functional thermochemistry. III. The role of exact exchange. *J. Chem. Phys.* **98**, 5648-5652 (1993).

(2) Tomasi, J.; Mennucci, B.; & Cammi, R. Quantum mechanical continuum solvation models, *Chem. Rev.* **105**, 2999-3093 (2015).

(3) Frisch, M. J.; Trucks, G. W.; Schlegel, H. B.; Scuseria, G. E.; Robb, M. A.; Cheeseman, J. R.; Scalmani, G.; Barone, V.; Petersson, G. A.; Nakatsuji, H.; Li, X.; Caricato, M.; Marenich, A. V.; Bloino, J.; Janesko, B. G.; Gomperts, R.; Mennucci, B.; Hratchian, H. P.; Ortiz, J. V.; Izmaylov, A. F.; Sonnenberg, J. L.; Williams-Young, D.; Ding, F.; Lipparini, F.; Egidi, F.; Goings, J.; Peng, B.; Petrone, A.; Henderson, T.; Ranasinghe, D.; Zakrzewski, V. G.; Gao, J.; Rega, N.; Zheng, G.; Liang, W.; Hada, M.; Ehara, M.; Toyota, K.; Fukuda, R.; Hasegawa, J.; Ishida, M.; Nakajima, T.; Honda, Y.; Kitao, O.; Nakai, H.; Vreven, T.; Throssell, K.; Montgomery, J. A., Jr.; Peralta, J. E.; Ogliaro, F.; Bearpark, M. J.; Heyd, J. J.; Brothers, E. N.; Kudin, K. N.; Staroverov, V. N.; Keith, T. A.; Kobayashi, R.; Normand, J.; Raghavachari, K.; Rendell, A. P.; Burant, J. C.; Iyengar, S. S.; Tomasi, J.; Cossi, M.; Millam, J. M.; Klene, M.; Adamo, C.; Cammi, R.; Ochterski, J. W.; Martin, R. L.;

Morokuma, K.; Farkas, O.; Foresman, J. B.; & Fox, D. J. Gaussian 16, Revision B.01, *Gaussian, Inc., Wallingford CT* (2016).

(4) O'Boyle, N. M.; Tenderholt, L. A. & Langner, K. M. cclib: A library for package-independent computational chemistry algorithms. *J. Comput. Chem.* **29**, 839–845 (2008).